A Hamiltonian approach to the parametric excitation

2006 Eur. J. Phys. 27 469

(http://iopscience.iop.org/0143-0807/27/3/001)

INSTITUTE OF PHYSICS PUBLISHING EUROPEAN JOURNAL OF PHYSICS

Eur. J. Phys. **27** (2006) 469–483 doi:10.1088/0143-0807/27/3/001

A Hamiltonian approach to the parametric excitation

V Leroy[1,2,3], J-C Bacri[1,2], T Hocquet[1,2] and M Devaud[1,2]

[1] Laboratoire Matière et Systèmes complexes, Université Denis Diderot—Paris 7, 140 rue de Lourmel, 75015 Paris, France
[2] CNRS UMR 7057, Paris, France

E-mail: valentin.leroy@loa.espci.fr

Received 1 April 2005, in final form 22 December 2005
Published 28 February 2006
Online at stacks.iop.org/EJP/27/469

Abstract

We propose a solution of the parametrically excited oscillator problem using the Hamiltonian formalism introduced by Glauber. The main advantage is that, within the framework of this formalism, the different possible approximations appear much more naturally than in the standard textbook presentation. Experiments on adiabatic and resonant parametric excitations of a pendulum are presented as an illustration, with particular attention being paid to the role played by the phase of the excitation.

1. Introduction

Parametric oscillators have a large number of applications, especially in electronics and optics [1]. Their study also provides a good introduction to parametric instability as the Faraday instability for instance. The pedagogical interest of the subject is at the origin of a wealth of publications and one can find a lot of papers proposing original experimental devices [2]. Nevertheless, although these devices are rather simple and allow students an easy familiarization with parametric oscillators, the theoretical explanation is generally either elusive or cumbersome.

In this respect, let us briefly recall the usual textbook treatment of the problem [3, 4]. One is interested in the motion of a harmonic oscillator one or several parameters of which are varied in the course of time. The most common example is that of a pendulum, the hanging point of which undergoes a periodic vertical displacement, leading to a time variation of apparent gravity $g(t)$. The equation of the motion then reads

$$\ddot{\theta} + \omega^2(t)\theta = 0, \tag{1}$$

where θ is the (small) angle between the vertical and the pendulum and $\omega(t) = \sqrt{g(t)/\ell}$ is the time-dependent angular frequency, ℓ standing for the pendulum length. If g follows

[3] Present address: Department of Physics Astronomy University of Manitoba, Winnipeg MB R3T 2N2, Canada.

a sinusoidal modulation of the type $g(t) = g_0(1 + \epsilon_g \sin \Omega t)$, equation (1) is known as the Mathieu equation [5]. At this step, the standard approach consists of declaring that a parametric resonance occurs for $\Omega = 2\omega$ and to look for a solution of the form

$$\theta(t) = a(t) \cos \frac{\Omega t}{2} + b(t) \sin \frac{\Omega t}{2},$$

with $\Omega \simeq 2\omega$ and where $a(t)$ and $b(t)$ are slowly varying functions of time. This procedure is of course perfectly correct, but not intuitive at first sight and often rather puzzling for undergraduate students. As a matter of fact, the appearance of a resonance for $\Omega = 2\omega$ is not straightforward from equation (1).

We propose in this paper an alternative approach based on the Hamiltonian formalism. The idea is to substitute a first-order but complex equation for equation (1) which is real but of second order. It will then be possible to express the solution in an integral form, which will suggest the well-founded approximations to be made in a very natural way. This paper is organized as follows. In section 2, we establish the equations of a parametrically excited harmonic oscillator using the Hamiltonian formalism. On this occasion, we introduce the Glauber variables and the secular approximation. Section 3 is devoted to the experimental device we used to illustrate the theoretical results. Section 4 deals with the *adiabatic* parametric excitation: we solve the motion equations of section 2 in the case of a harmonic oscillator a parameter of which is slowly varied, and we present an experimental illustration. Section 5 is concerned with the *resonant* parametric excitation. We present a complete discussion of the solution, overstepping the usual mere determination of the instability threshold (which can also be done using the standard approach). In particular, we emphasize the role played by the dephasing between the pendulum oscillation and the parametric excitation itself.

2. The Hamiltonian resolution

We shall now establish the first-order complex differential equation to be substituted for equation (1). Since our experimental implementation uses a pendulum device, which is, by the way, the most studied paradigm of the parametric oscillator, our calculations will therefore be carried out using the pendulum example. Of course, they could also be applied to any other type of parametrically excited harmonic oscillator.

2.1. The Glauber variable

To begin with, let us write down the equation of the problem. The dynamical variable is naturally chosen to be angle θ. Let J be the inertia momentum with respect to the oscillation axis, ℓ the distance between the centre of mass and this axis, and M the total mass of the pendulum. A Lagrangian of the system is

$$L = \tfrac{1}{2} J \dot{\theta}^2 - Mg\ell(1 - \cos\theta). \tag{2}$$

We will only consider small oscillations, allowing us to substitute $\frac{1}{2}\theta^2$ for $1 - \cos\theta$ into the above equation. Furthermore, it will be convenient to introduce the new dynamical variable $q = \sqrt{J}\theta$. Then, from the new Lagrangian

$$L = \tfrac{1}{2}(\dot{q}^2 - \omega^2 q^2), \tag{3a}$$

with $\omega = \sqrt{Mg\ell/J}$, we can build the Hamiltonian

$$H = \tfrac{1}{2}(p^2 + \omega^2 q^2), \tag{3b}$$

where p is the conjugate momentum of dynamical variable q. Hamilton's equations read $\dot{q} = \frac{\partial H}{\partial p} = p$, $\dot{p} = -\frac{\partial H}{\partial q} = -\omega^2 q$, which combine in the dissipation-free motion equation $\ddot{q} + \omega^2 q = 0$.

One can then try to merge both Hamilton's equations in a unique first-order equation. With this aim, one has to build an *ad hoc* complex variable. Let us take for instance the dimensionless Glauber variable α defined as

$$\alpha = \frac{1}{\sqrt{2\hbar}} \left(\sqrt{\omega} q + \frac{\mathrm{i}}{\sqrt{\omega}} p \right), \tag{4}$$

where $\hbar$ is the usual quantum constant[4]. Of course, in our problem, everything is classical and $\hbar$ should *in fine* disappear from any relevant motion equation. We nevertheless keep Glauber's definition (4) for it provides an interesting bridge with quantum mechanics. Expressed in terms of α, Hamiltonian H reads:

$$H = \hbar\omega |\alpha|^2. \tag{5}$$

The dimensionless quantity $|\alpha|^2$ can thus be regarded as the number N of (semi-classical) oscillation quanta. Moreover, the Poisson bracket $\{\alpha, \alpha^*\} = \frac{\partial \alpha}{\partial q}\frac{\partial \alpha^*}{\partial p} - \frac{\partial \alpha}{\partial p}\frac{\partial \alpha^*}{\partial q}$ being equal to $\frac{1}{\mathrm{i}\hbar}$, the equation verified by α is independent of the numerical value of $\hbar$, as expected for a classical result; it reads

$$\dot{\alpha} = \{\alpha, H\} = -\mathrm{i}\omega\alpha \quad \rightsquigarrow \quad \alpha(t) = \alpha(0)\, \mathrm{e}^{-\mathrm{i}\omega t}. \tag{6}$$

So $|\alpha(t)|^2 = |\alpha(0)|^2$: the quanta number is a constant of the motion, which, allowing for equation (5), contains the energy conservation in the dissipation-free movement. In the complex plane of the Glauber variable α, the trajectory of the representative point (the 'phase portrait') is a circle, with centre at the origin and followed clockwise uniformly.

2.2. The secular approximation

The simple *free* motion equation (6) of the oscillator naturally becomes involved when more complex situations or phenomena are envisaged. For example, let us take dissipation into account. In most textbooks [8], only viscous friction is considered, whereas solid friction is often the dominant damping mechanism (as is the case with our pendulum device). However that may be, since dissipation does not play a major role in our experimental discussion, we shall use hereafter the simple viscous friction law for the sake of simplicity. Let us, therefore, add the phenomenological $-\gamma\dot{q}(= -\gamma p)$ viscous friction term to the right-hand side of the second of Hamilton's equations. Keeping definition (4) of α unchanged, we easily get

$$\dot{\alpha} = \frac{1}{\sqrt{2\hbar}} \left(\sqrt{\omega} p + \frac{\mathrm{i}}{\sqrt{\omega}} (-\omega^2 q - \gamma p) \right) = -\mathrm{i}\omega\alpha - \frac{\gamma}{2}(\alpha - \alpha^*). \tag{7}$$

Equation (7) is not difficult to solve, despite the α^* term on its right-hand side. Its exact solution is, as can easily be checked,

$$\alpha(t) = \mathrm{e}^{-\frac{\gamma t}{2}} \left[\alpha(0) \left(\cos\omega' t - \mathrm{i}\frac{\omega}{\omega'} \sin\omega' t \right) + \frac{\gamma}{2\omega'} \alpha^*(0) \sin\omega' t \right], \tag{8a}$$

with

$$\omega' = \sqrt{\omega^2 - \frac{\gamma^2}{4}}. \tag{8b}$$

[4] Glauber [6] introduced his formalism in the quantum mechanics domain, when aiming to describe the quasi-classical ('coherent') states of the HO. Hence the presence of the quantum constant $\hbar$ in the definition itself of α, which is just the classical transposition of the boson annihilation operator a: α is thus, unfortunately, often associated with *mere* quantum mechanics. For more details, see [7].

Provided that the damping is weak enough (i.e. $\gamma \ll \omega$), the exact expression (8*a*) can be approximated by

$$\alpha(t) \simeq \alpha(0)\, \mathrm{e}^{-\frac{\gamma t}{2}}\, \mathrm{e}^{-\mathrm{i}\omega t}. \tag{9}$$

It is remarkable that the above approximate solution (9) is exactly what is obtained when neglecting the α^* term on the right-hand side of equation (7). This can be understood as follows. Let us set up a perturbative resolution of this equation, with damping being regarded as the perturbation. The zero-order (i.e. unperturbed) solution, as displayed in equation (6), is $\alpha(t) = A\, \mathrm{e}^{-\mathrm{i}\omega t}$, where A is a constant. Damping is then taken into account by allowing A to vary *slowly*, i.e. at a rate typically of order of γ, which yields

$$\dot{A} = -\frac{\gamma}{2}(A - A^*\, \mathrm{e}^{2\mathrm{i}\omega t}). \tag{10}$$

In equation (10), the oscillations of the $\mathrm{e}^{2\mathrm{i}\omega t}$ phase factor average to zero the A^* term's contribution to the time evolution of A, as can be seen by the time integration

$$A(t) = A(0) - \frac{\gamma}{2}\int_0^t \mathrm{d}t'(A(t') - A^*(t')\, \mathrm{e}^{2\mathrm{i}\omega t'}). \tag{11}$$

The above equation is satisfied by $A(t) = A(0)\, \mathrm{e}^{-\frac{\gamma t}{2}}$, provided that condition $\frac{\gamma}{2} \ll \left|2\mathrm{i}\omega - \frac{\gamma}{2}\right|$ (i.e. $\gamma \ll \omega$) is fulfilled, which we assume. *In fine*, equation (10) can be simplified in $\dot{A} = -\frac{\gamma}{2}A$, and the approximate result (9) is directly obtained. Neglecting the A^* term on the right-hand side of (10) is known as the secular approximation (SA). We shall use it frequently throughout the present paper.

At the SA, and as a consequence of result (9), the oscillation quanta number $N = |\alpha|^2$ decays exponentially with the rate γ. Thus, in the complex plane of Glauber variable α, due to the weak viscous friction, the circular phase portrait is changed into a uniformly followed logarithmic spiral (with centre at the origin).

2.3. Parametric excitation

Let us consider now how the free motion equation (6) of the pendulum is modified when one of its parameters is changed in the course of the oscillation. This parameter can be either gravity g or length ℓ. The former situation can be simulated, as seen in the introduction, by an *ad hoc* acceleration (up or down) of the oscillation axis. The linearized Lagrangian (2) then reads

$$L(t) = \tfrac{1}{2}(J\dot{\theta}^2 - Mg(t)\ell\theta^2), \tag{12}$$

and we obtain the motion equation (1) with $\omega(t) = \sqrt{Mg(t)\ell/J}$.

The second possible parametric excitation is achieved when changing ℓ (and consequently J, which is roughly equal to $M\ell^2$) and gives the Lagrangian

$$L(t) = \tfrac{1}{2}(J(t)\dot{\theta}^2 - Mg\ell(t)\theta^2), \tag{13}$$

which leads to

$$\frac{1}{J}\frac{\mathrm{d}}{\mathrm{d}t}(J\dot{\theta}) + \omega^2(t)\theta = 0, \qquad \text{with} \qquad \omega(t) = \sqrt{\frac{Mg\ell(t)}{J(t)}}. \tag{14}$$

It should be noted that changing g or ℓ does not lead to the same motion equation[5].

[5] In fact, equation (14) can be given the same *form* as (1) by substituting variable τ, defined by $\mathrm{d}\tau = \mathrm{d}t/J(t)$, for time t. We then get $\frac{\mathrm{d}^2\theta}{\mathrm{d}\tau^2} + (J\omega)^2(\tau)\theta = 0$ (see, for instance, [4]). Nevertheless, such a 'time dilatation' should rather be regarded as an artful mathematical trick.

Let us now perform a Legendre transformation of Lagrangians (12) and (13). In both cases we get:

$$H(t) = \frac{\sigma^2}{2J} + \frac{1}{2}Mg\ell\theta^2, \tag{15}$$

where $\sigma = J(t)\dot{\theta}$ stands for the conjugate momentum of angle θ, and where either g or (J, ℓ) depends on time. It is noteworthy that expression (3*b*) of Hamiltonian $H(t)$ is still valid, with $q = \sqrt{J}\theta$ and $p = \frac{\sigma}{\sqrt{J}} (\neq \dot{q})$. As a consequence, with definition (4) of α generalized in

$$\alpha(t) = \frac{1}{\sqrt{2\hbar}} \left(\sqrt{(J\omega)(t)}\theta + \frac{\mathrm{i}}{\sqrt{(J\omega)(t)}}\sigma \right), \tag{16}$$

this Hamiltonian reads

$$H(t) = \hbar\omega(t)|\alpha(t)|^2, \tag{17}$$

and the free motion equation (6) becomes

$$\dot{\alpha}(t) = \{\alpha, H\} + \frac{\partial\alpha}{\partial t} = -\mathrm{i}\omega(t)\alpha + f(t)\alpha^*, \tag{18a}$$

where

$$f(t) = \frac{(\dot{J\omega})}{2J\omega} = \frac{\mathrm{d}}{\mathrm{d}t} \ln \sqrt{(J\omega)(t)}. \tag{18b}$$

In order to simultaneously allow for a *weak* viscous damping and a parametric excitation of the pendulum, equations (7) (on the right-hand side of which the nonsecular $\frac{\gamma}{2}\alpha^*$ viscous term is henceforth neglected) and (18*a*) are combined into

$$\dot{\alpha} = -\mathrm{i}\omega(t)\alpha - \frac{\gamma}{2}\alpha + f(t)\alpha^*. \tag{19}$$

Observe that both kinds of parametric excitation lead to the *same* motion equation (19) for the Glauber variable α. Let us focus, for example, on the case of a small sinusoidal length modulation:

$$\ell(t) = \ell_0(1 + \epsilon \sin(\Omega t + \varphi)), \tag{20}$$

with $\epsilon \ll 1$. We introduce a phase φ in view of analysing, as announced in the introduction, its influence on the motion of the pendulum. When the length is modulated following (20), $J(t)$ and $\omega(t)$ are also modulated

$$J(t) = J_0(1 + \epsilon_J \sin(\Omega t + \varphi)), \tag{21}$$

$$\omega(t) = \omega_0(1 + \epsilon_\omega \sin(\Omega t + \varphi)), \tag{22}$$

and $f(t)$ reads

$$f(t) = \epsilon_f \Omega \cos(\Omega t + \varphi), \tag{23}$$

where ϵ_J, ϵ_ω and $\epsilon_f = \frac{1}{2}(\epsilon_J + \epsilon_\omega)$ can be calculated as functions of ϵ. For a simple pendulum, $J = M\ell^2$ and we have $\epsilon_J = 2\epsilon$, $\epsilon_\omega = -\epsilon/2$ and $\epsilon_f = 3\epsilon/4$.

3. Experimental details

3.1. The experimental device

A sketch of the pendulum we used for the experiments is displayed in figure 1. This pendulum is made of a couple of light parallel metallic rods with mass m. A heavy cylinder with mass M_c can be slid along the rods. The whole set can rotate freely around one horizontal axis (A) thanks to ball-bearings. The position of the pendulum is defined by the angle θ that the rods

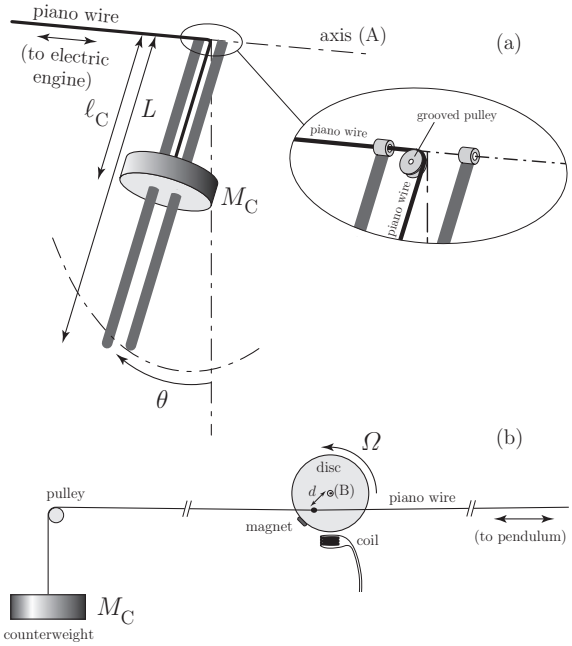

Figure 1. Experimental device. (a) The pendulum can rotate freely around axis (A). The cylindrical mass M_C is held, and can be slid, along a couple of rods thanks to a piano wire through a grooved pulley in such a way that no torque at all is exerted upon (A). (b) The piano wire's second extremity is fastened on a vertical disc at a distance d from its horizontal axis (B). The disc's rotation is carried out by an electric engine and facilitated by a counterweight system. The phase of the disc's rotation is marked thanks to a magnet–coil device.

make with the vertical. This angle is measured by means of a potentiometric device connected to a numerical oscilloscope (not shown in the figure).

The cylinder is held, and slid along the rods, thanks to a piano wire dragged through a grooved pulley located on axis (A), so that no torque at all is exerted onto this axis by the wire's doing: moving mass M_c along the rods simply changes its distance ℓ_c to axis (A) and should thus be regarded as a pure parametric excitation of the pendulum. In our experiment, we perform a sinusoidal modulation of length ℓ_c. With this aim, the second extremity of the piano wire is fastened on a vertical disc, at a distance d from its (horizontal) axis (B). An electric engine rotates the disc at any desired angular frequency Ω. The disc is placed far enough from the pendulum for length $\ell_c(t)$ to be consequently ruled by $\ell_c(t) = \ell_{c0} + d \sin \Omega t$. In order to mark the phase of the disc rotation, we glued a small magnet on its edge and put a coil under the disc, at the vertical of its axis (B) (see (b) in figure 1). The disc being rotated counterclockwise, we thus obtain a peak voltage roughly when the cylinder is at its mean position ($\ell_c = \ell_{c0}$) and descending. Let us add that in order to balance the torque exerted by the cylinder weight onto axis (B), and hence to facilitate the engine rotation, we disposed the counterweight device displayed in the figure. The characteristics of the pendulum are listed in table 1.

3.2. Deviation from simplicity

Our pendulum is clearly not simple and we will need to account for this non-simplicity in our calculus when we want to compare the experimental results with the theory. The first

Table 1. Characteristics of the pendulum.

Length of the rods	L	82.2 cm ± 2 mm
Height of the cylinder	h	2 cm ± 1 mm
Radius of the cylinder	R	5.2 cm ± 1 mm
Mass of the rods	m	177 g ± 5 g
Mass of the cylinder	M_c	1.38 kg ± 10 g

difference with the simple pendulum is that we modulate ℓ_c and not ℓ directly. Let us note

$$\ell_c(t) = \ell_{c0}(1 + \epsilon_c \sin(\Omega t + \varphi)). \tag{24}$$

The modulation depth ϵ_c depends on parameters d and ℓ_{c0} of the device displayed in figure 1: $\epsilon_c = \frac{d}{\ell_{c0}}$. When the cylinder moves, it moves the centre of mass, $M\ell(t) = 2 \times \frac{1}{2}mL + M_c\ell_c(t)$, with $M = 2m + M_c$. We consequently have

$$\epsilon = \frac{M_c\ell_{c0}}{M\ell_0}\epsilon_c. \tag{25}$$

Furthermore, J is not equal to $M\ell^2$ but reads $J = M_c\left(\ell_c^2 + \frac{R^2}{2} + \frac{h^2}{12}\right) + \frac{2}{3}mL^2$. We then obtain

$$\epsilon_J = 2\frac{M_c\ell_{c0}^2}{J_0}\epsilon_c. \tag{26}$$

It follows that we have

$$\epsilon_\omega = \frac{1}{2}(\epsilon - \epsilon_J) = \frac{1}{2}\left(\frac{M_c\ell_{c0}}{M\ell_0} - 2\frac{M_c\ell_{c0}^2}{J_0}\right)\epsilon_c, \tag{27}$$

and

$$\epsilon_f = \frac{1}{2}(\epsilon_J + \epsilon_\omega) = \frac{1}{4}\left(\frac{M_c\ell_{c0}}{M\ell_0} + 2\frac{M_c\ell_{c0}^2}{J_0}\right)\epsilon_c. \tag{28}$$

4. Adiabatic parametric excitation

4.1. Mathematical resolution

Let us consider a *slow* (adiabatic in the Ehrenfest sense) variation of whichever parameter (g or ℓ). This means that the parameter and its time derivatives have small variations on the time scale of one period $\frac{2\pi}{\omega}$ of the free oscillations, which can be summarized in the following twofold condition. On the one hand $|f(t)| \ll \omega$ and, on the other hand, all nonzero components of the Fourier spectrum of $f(t)$ correspond to angular frequencies well *below* ω. If this condition is fulfilled, the same arguments as in subsection (2.2) (when discussing the relevance of keeping the $\frac{\gamma}{2}\alpha^*$ term on the right-hand side of equation (7)) hold: the $\frac{\partial\alpha}{\partial t} = f(t)\alpha^*$ term in equation (19) brings no secular contribution to the time evolution of $\alpha(t)$, which reads *in fine* at the SA:

$$\alpha(t) = \alpha(0)\,\mathrm{e}^{-\frac{\gamma}{2}t}\,\mathrm{e}^{-\mathrm{i}\beta(t)}, \tag{29a}$$

with

$$\beta(t) = \int_0^t \mathrm{d}t'\omega(t'). \tag{29b}$$

The phase portrait is then a logarithmic spiral, still followed clockwise, but no longer uniformly. Let us provisionally neglect dissipation: the above spiral becomes a circle. The quanta number

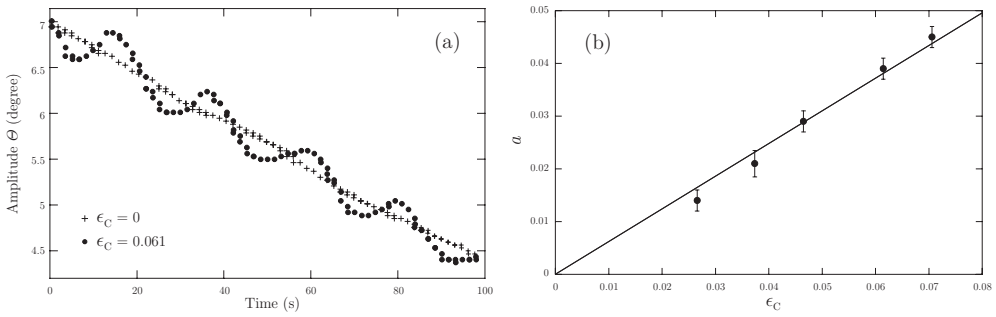

Figure 2. (a) Decay of the oscillation maximum amplitude $\Theta(t)$ without (+, $\epsilon_c = 0$) and with (•, $\epsilon_c = 0.061$) pendulum length modulation. (b) Fitted parameter a (as explained in the text) as a function of the experimental modulation depth ϵ_c. The slope of the solid straight line is 0.62 ± 0.02, to be compared with the 0.64 theoretically predicted value.

$N = |\alpha|^2$ is therefore an adiabatic invariant of the undamped movement. Let Θ be the maximum amplitude of the oscillation. The slowly varying total energy of the oscillator reads

$$\mathcal{E}(t) = \tfrac{1}{2} J(t)\omega^2(t)\Theta^2(t). \tag{30a}$$

Allowing for (17) and (29*a*) with $\gamma = 0$, we get

$$|\alpha|^2 = \frac{\mathcal{E}(t)}{\hbar\omega(t)} = \frac{1}{2\hbar} J(t)\omega(t)\Theta^2(t) = \text{cst}, \tag{30b}$$

so that Θ varies like $(J\omega)^{-1/2}$. It is noteworthy that this result holds even if parameter g or ℓ is varied over a wide range (provided that $|\Theta| \ll 1$). Nevertheless, for the convenience of our experimental implementation, we shall consider hereafter a small modulation depth ϵ, as in equation (20). If $\Omega \ll \omega$, the SA is valid and the expected variation of Θ is then

$$\Theta(t) = \Theta_0\big(1 - \tfrac{1}{2}(\epsilon_\omega + \epsilon_J)\sin(\Omega t + \varphi)\big), \tag{31}$$

which reduces to

$$\Theta(t) = \Theta_0\big(1 - \tfrac{3}{4}\epsilon \sin(\Omega t + \varphi)\big) \tag{32}$$

for a simple pendulum.

4.2. Experimental illustration

Let us recall that the pendulum we use in our experiment is not simple, with *inter alia* the consequence that we do not modulate ℓ directly but ℓ_c, with a modulation depth $\epsilon_c = \frac{d}{\ell_{c0}}$ (see figure 1).

Figure 2(a) displays the evolution of Θ as a function of time, with and without modulation. When there is no length modulation ($\epsilon_c = 0$), we observe a linear damping which is well fitted by the law, $\Theta = \Theta_0 - rt$, with a linear decay rate $r = 2.6 \times 10^{-2}$ deg s^{-1}. In the case of length modulation (here $\epsilon_c = 0.061$ and $\Omega \simeq 0.07\omega$), we observe a low frequency modulation of Θ superimposed to the linear damping. We can fit these data with

$$\Theta(t) = (\Theta_0 - rt)(1 - a\sin\Omega t), \tag{33}$$

where the values of r and Ω are known, and that of a is determined by the fit.

Figure 2(b) displays the fitted parameter a as a function of the experimental modulation depth ϵ_c. We obtain a straight line, with a slope of 0.62 ± 0.02. Now, according to (31), we expect $a = \epsilon_f$. The calculus detailed in 3.2 allows us to estimate, knowing the characteristics of the pendulum (see table 1) and the mean position of the cylinder ($\ell_{c0} = 60.2$ cm $\pm$ 2 mm), that $\epsilon_f = 0.64\epsilon_c$. So, the agreement is satisfactory.

5. Resonant parametric excitation

5.1. Mathematical resolution

We now come back to the general equation (19), and consider a situation in which the $f(t)\alpha^*$ term on the right-hand side brings in a secular contribution to the time evolution of α. A perturbative resolution is then set up, modifying equations (29) in

$$\alpha(t) = A(t)\,\mathrm{e}^{-\frac{\gamma}{2}t}\,\mathrm{e}^{-\mathrm{i}\beta(t)}. \tag{34}$$

Without parametric excitation, $A(t)$ would be the constant $A(0) = \alpha(0)$. Due to the excitation, it is the solution of the differential equation

$$\dot{A} = f(t)\,\mathrm{e}^{2\mathrm{i}\beta(t)}A^*. \tag{35}$$

The phase factor $\mathrm{e}^{2\mathrm{i}\beta(t)}$ can be expanded as follows:

$$\mathrm{e}^{2\mathrm{i}\beta(t)} = \mathrm{e}^{2\mathrm{i}\omega_0 t}\left(1 + 2\mathrm{i}\epsilon_\omega\frac{\omega_0}{\Omega}(1 - \cos(\Omega t + \varphi)) + \cdots\right). \tag{36}$$

Moreover, when expanding $f(t)$ also, function $f(t)\,\mathrm{e}^{2\mathrm{i}\beta(t)}$ is of the general form

$$f(t)\,\mathrm{e}^{2\mathrm{i}\beta(t)} = \Omega\sum_{n=-\infty}^{+\infty} c_n\,\mathrm{e}^{\mathrm{i}(2\omega_0 - n\Omega)t - \mathrm{i}n\varphi}, \tag{37}$$

where coefficients c_n can be calculated as functions of ϵ_ω and ϵ_f. The right-hand side of equation (35) therefore gives a secular contribution to the time evolution of A only for a discrete series of values of Ω, namely $\Omega_n = \frac{2\omega_0}{n}$, with $n = 1, 2, 3, \ldots$. These values are the resonant parametric excitation angular frequencies. At *first order* in the modulation depth ϵ, the only nonzero coefficient c_n in (37) is $c_1 = \frac{\epsilon_f}{2}$. The main resonance is thus obtained for $\Omega = 2\omega_0$. Higher order resonances ($n = 2, 3, \ldots$) are but the consequence of harmonic generation in the full expansions of $\omega(t)$, $\beta(t)$, $f(t)$ and $\mathrm{e}^{2\mathrm{i}\beta(t)}$. In this sense, they can be regarded as 'secondary'. In our experimental check, we shall focus on the 'primary' $n = 1$ resonance. Nevertheless, by care of generality, we write the following theoretical treatment in such a way that it can also apply to any integer value of n. Setting

$$2\delta_n = n\Omega - 2\omega_0, \qquad \varphi_n = n\varphi \tag{38}$$

and assuming $|\delta_n| \ll \omega_0$, equation (35) reads at the SA,

$$\dot{A} = \Omega c_n\,\mathrm{e}^{-2\mathrm{i}\delta_n t - \mathrm{i}\varphi_n}A^*. \tag{39}$$

Then, henceforth omitting index n in c_n, φ_n and δ_n, and setting $A = B\,\mathrm{e}^{-\mathrm{i}\delta t}$ with $B(0) = A(0) = \alpha(0)$, equation (39) becomes

$$\dot{B} = \mathrm{i}\delta B + \Omega c\,\mathrm{e}^{-\mathrm{i}\varphi}B^*. \tag{40}$$

Writing $B = X + \mathrm{i}Y$ and $c\,\mathrm{e}^{-\mathrm{i}\varphi} = c' + \mathrm{i}c''$, equation (40) is turned into the linear system:

$$\begin{bmatrix}\dot{X}\\ \dot{Y}\end{bmatrix} = \mathbb{M}\begin{bmatrix}X\\ Y\end{bmatrix}, \qquad \text{with} \qquad \mathbb{M} = \begin{pmatrix}\Omega c' & \Omega c'' - \delta\\ \Omega c'' + \delta & -\Omega c'\end{pmatrix}. \tag{41}$$

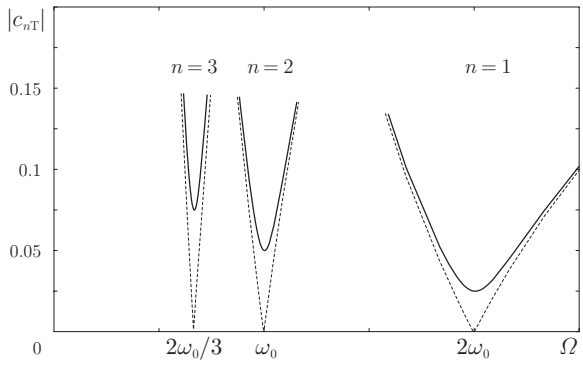

Figure 3. Threshold values $|c_n\mathrm{T}|(\Omega)$ for the parametric amplification for the $n = 1$, $n = 2$ and $n = 3$ resonances (dotted lines: $\gamma = 0$; solid lines: $\gamma \neq 0$). If $|c| < |c_\mathrm{T}|(\Omega)$, any initial oscillation dies out when $t \to \infty$. If $|c| > |c_\mathrm{T}|(\Omega)$, an initial oscillation of the pendulum may be exponentially amplified.

This system is easily solved using standard methods. Let $\pm\lambda$ be the eigenvalues of matrix $\mathbb{M}$ ($\lambda^2 = \Omega^2|c|^2 - \delta^2$). The solution of (40) reads, all calculations carried out,

$$B(t) = B_+(t) + B_-(t) = \alpha_+(0)\,\mathrm{e}^{\lambda t} + \alpha_-(0)\,\mathrm{e}^{-\lambda t} \tag{42}$$

with

$$\begin{aligned} \alpha_+(0) &= \frac{1}{2\lambda}[(\lambda + \mathrm{i}\delta)\alpha(0) + \Omega c\,\mathrm{e}^{-\mathrm{i}\varphi}\alpha^*(0)], \\ \alpha_-(0) &= \frac{1}{2\lambda}[(\lambda - \mathrm{i}\delta)\alpha(0) - \Omega c\,\mathrm{e}^{-\mathrm{i}\varphi}\alpha^*(0)]. \end{aligned} \tag{43}$$

Then, one can go back to the expression of $\alpha(t) = \alpha_+(t) + \alpha_-(t)$, with

$$\alpha_\pm(t) = \alpha_\pm(0)\,\mathrm{e}^{(\pm\lambda - \frac{\gamma}{2})t}\,\mathrm{e}^{-\mathrm{i}(\frac{n\Omega t}{2} + \beta(t) - \omega_0 t)}. \tag{44}$$

It is noteworthy that, as suggested by (36), the phase factor $\mathrm{e}^{\mathrm{i}(\omega_0 t - \beta(t))}$ can be approximated by unity if $|\epsilon_\omega| \ll 1$. We then obtain the approximate expression

$$\alpha(t) \simeq \alpha_+(0)\,\mathrm{e}^{(+\lambda - \frac{\gamma}{2})t}\,\mathrm{e}^{-\mathrm{i}\frac{n\Omega t}{2}} + \alpha_-(0)\,\mathrm{e}^{(-\lambda - \frac{\gamma}{2})t}\,\mathrm{e}^{-\mathrm{i}\frac{n\Omega t}{2}}. \tag{45}$$

5.2. The different regimes

From the above result (42), two regimes are possible, according to $\Omega|c|$ being smaller or larger than $|\delta|$.

(i) If $\Omega|c| < |\delta|$, then $\lambda = \mathrm{i}\sqrt{\delta^2 - \Omega^2|c|^2}$ is *imaginary* and function $B(t)$ oscillates with angular frequency $\sqrt{\delta^2 - \Omega^2|c|^2}$.[6]

(ii) If $\Omega|c| > |\delta|$, then $\lambda = \sqrt{\Omega^2|c|^2 - \delta^2}$ is *real* and $B(t)$ is the sum of two terms with constant arguments, the former growing like $\mathrm{e}^{\lambda t}$, the latter decaying like $\mathrm{e}^{-\lambda t}$.

Therefore, if we want a parametric instability to spread out, we must try to be in regime (ii), which we assume in this subsection. Moreover, the growing rate λ should be large enough

[6] By way of a check, observe that in the limit case $|c| = 0$ (i.e. when no parametric excitation is implemented at all), we have $\beta(t) = \omega_0 t$, $\lambda = \mathrm{i}|\delta|$, $B(t) = \alpha(0)\,\mathrm{e}^{\mathrm{i}\delta t}$, and thus (9) is recovered from (44), as expected.

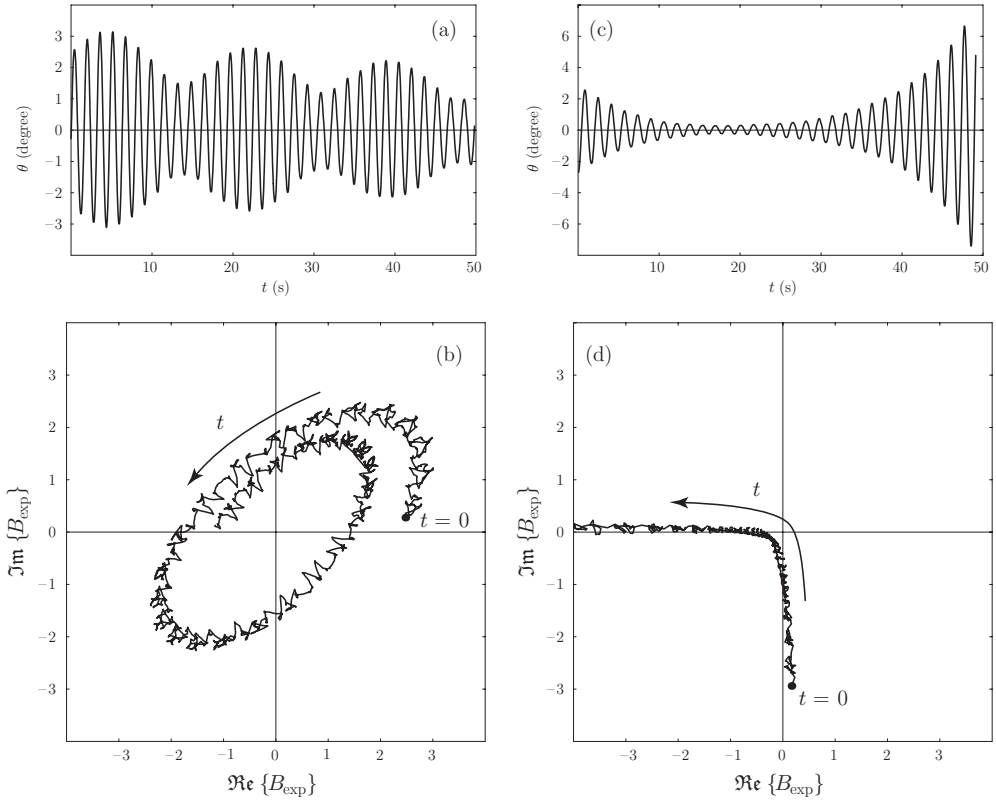

Figure 4. Left: regime (i). (a) Measured oscillation angle θ as a function of time. (b) Trajectory of variable $B_{\rm exp}(t)$ in the complex plane. Right: regime (ii). (c) Measured oscillation angle θ as a function of time. (d) Trajectory of variable $B_{\rm exp}(t)$ in the complex plane.

to make up for the dissipation. Thus, at a given Ω, threshold values $c_{n\rm T}$ for the parametric amplification to occur are defined by

$$\lambda_{\rm T} = \sqrt{\Omega^2|c_{n\rm T}|^2 - \delta_n^2} = \frac{\gamma}{2} \tag{46}$$

$$\rightsquigarrow |c_{n\rm T}| = \frac{1}{\Omega}\sqrt{\left(\frac{n\Omega}{2} - \omega_0\right)^2 + \frac{\gamma^2}{4}} \simeq \frac{n}{2\omega_0}\sqrt{\left(\frac{n\Omega}{2} - \omega_0\right)^2 + \frac{\gamma^2}{4}}. \tag{47}$$

Consequently, as is well known [9], the curve $|c_{n\rm T}|(\Omega)$ separates, in the vicinity of abscissa $\Omega_n = \frac{2\omega_0}{n}$, the $(|c_n|, \Omega)$ plane into two domains: beneath this curve, an initial oscillation ($\alpha(0) \neq 0$) of the pendulum dies out whatever the $\alpha(0)$; above this curve, the amplitude may exponentially increase (until its growth is limited by some nonlinearity, the discussion of which is beyond the scope of the present paper). Curves $|c_{n\rm T}|(\Omega)$ are plotted in figure 4 for $n = 1, 2, 3$.

The above analysis shows that the instability is entirely controlled merely by parameters Ω and c. Nevertheless, phase φ is important too. In this respect, let us focus on primary resonance $n = 1$. At the first order, $c = c_1 = \frac{\varepsilon_f}{2}$ is real. We then have

$$\lambda + {\rm i}\delta = \Omega c\, {\rm e}^{{\rm i}\chi}, \quad \text{with } \cos\chi = \frac{\lambda}{\Omega c} \text{and } \sin\chi = \frac{\delta}{\Omega c}, \tag{48}$$

and numbers $\alpha_{\pm}(0)$ defined in (43) read

$$\alpha_{+}(0) = \frac{1}{\cos\chi}\,\mathrm{e}^{-\mathrm{i}\frac{\varphi-\chi}{2}}\,\mathrm{Re}\left\{\mathrm{e}^{\mathrm{i}\frac{\varphi+\chi}{2}}\alpha(0)\right\},$$
$$\alpha_{-}(0) = \frac{1}{\cos\chi}\,\mathrm{e}^{-\mathrm{i}\frac{\varphi+\chi}{2}}\,\mathrm{i}\,\mathrm{Im}\left\{\mathrm{e}^{\mathrm{i}\frac{\varphi-\chi}{2}}\alpha(0)\right\}. \tag{49}$$

When the solution is written in the above form, the role of phase φ is easily identified. Let us assume, for the sake of maximum simplicity, that we are exactly at resonance, i.e. $\chi = 0$. Then, allowing for (45) and (49), the growing part $\theta_{+}(t)$ of the solution oscillates in $\cos\left(\omega_0 t + \frac{\varphi}{2}\right)$. Owing to (24), this corresponds to $\ell_{\mathrm{c}} = \ell_{\mathrm{c}0}$ and $\dot{\ell}_{\mathrm{c}} = -2\omega_0\epsilon_{\mathrm{c}}\ell_{\mathrm{c}0}$, i.e. a *shortening* of the pendulum, when $\theta_{+} = 0$. On the other hand, the decaying part $\theta_{-}(t)$ of the solution oscillates in $\sin\left(\omega_0 t + \frac{\varphi}{2}\right)$; consequently, we have $\ell_{\mathrm{c}} = \ell_{\mathrm{c}0}$ and $\dot{\ell}_{\mathrm{c}} = 2\omega_0\epsilon_{\mathrm{c}}\ell_{\mathrm{c}0}$, i.e. a *lengthening* of the pendulum, for $\theta_{-} = 0$. The importance of this point can be easily shown on energetic grounds. Let us imagine a child going on a swing, flexing his knees and standing up straight periodically. If he stands up when the swing is at its lowest (i.e. vertical) position and flexes his knees when it is at a maximum amplitude, he will have to do some work: at the lowest position indeed the speed is maximum and he has to fight against a downward inertial force which reduces to zero when the swing stops at a maximum amplitude. Doing so, he *pumps* the swing (at actually an $\Omega = 2\omega_0$ angular frequency). On the other hand, if he dephases his movement, flexing his knees at the swing's lowest position and standing up at maximum amplitude, the opposite should happen: he *damps* the swing oscillation. A detailed discussion of this question (including departure from the ideal parametric excitation) can be found in [10].

The later evolution of the pendulum motion is determined at the very beginning by the initial dephasing between modulation and oscillation. In particular, if the initial oscillation phase is chosen such that $\mathrm{Re}\left\{\mathrm{e}^{\mathrm{i}\frac{\varphi}{2}}\alpha(0)\right\} = 0$, only the decreasing part $\alpha_{-}(t)$ of the solution is nonzero. There is then no instability, although parameters Ω and c are set for this instability to occur. Practically speaking, this situation is never observed because it is impossible to get $\alpha_{+}(0)$ exactly zero. Nevertheless, as shown in the next section, it is possible to approach this ideal situation, and observe temporarily a parametrically induced damping of the oscillation.

5.3. Experimental illustration

Let us now consider the experimental observations. We set $\ell_{\mathrm{c}0}$ to 67.1 cm $\pm$ 2 mm. Using the characteristics of the pendulum listed in table 1, we calculate the period $T_0 = 1.62 \pm 0.02$ s. The measured value is 1.62 s ($\omega_0 = 3.87$ rad s^{-1}). We calculate also $c_1 = \frac{\epsilon_f}{2} \simeq 0.33\epsilon_{\mathrm{c}}$. With an experimental length modulation depth $\epsilon_{\mathrm{c}} = 5 \times 10^{-2}$, we have therefore $c_1 = 1.65 \times 10^{-2}$. We choose the time origin to be the instant when the signal on the coil is maximum. Allowing for the experimental setup described in section 3, we therefore expect a length modulation with $\varphi \simeq 0$.

Figures 4(a) and (c) show the evolution of the measured angle θ as a function of time, for two different values of angular frequency Ω. From the $\theta(t)$ signal, we numerically construct $\dot{\theta}(t)$ and calculate the complex function α_{exp} defined as

$$\alpha_{\mathrm{exp}}(t) = \left(\theta(t) + \mathrm{i}\frac{\dot{\theta}(t)}{\omega_0}\right). \tag{50}$$

Function $\alpha_{\mathrm{exp}}(t)$ is, save a multiplicative factor, the Glauber variable $\alpha(t)$, defined in (16), into which, to be consistent at first order, ω_0 and J_0 are substituted for $\omega(t)$ and $J(t)$. From $\alpha_{\mathrm{exp}}(t)$, we then construct the complex function $B_{\mathrm{exp}}(t)$,

$$B_{\mathrm{exp}}(t) = \alpha_{\mathrm{exp}}(t)\,\mathrm{e}^{\mathrm{i}\frac{\Omega}{2}t}. \tag{51}$$

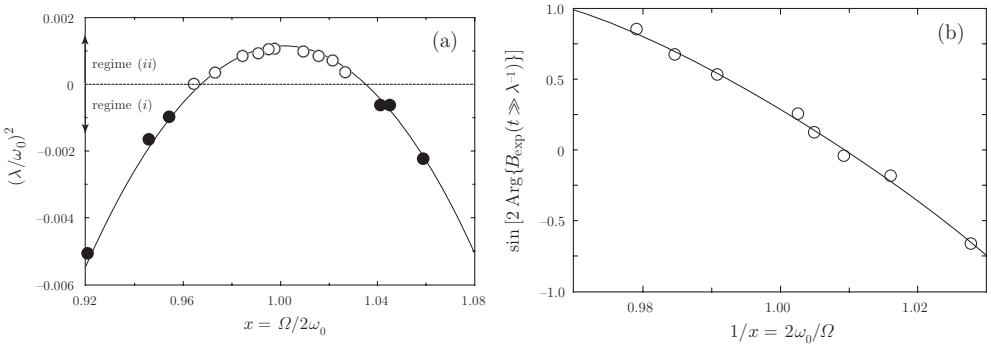

Figure 5. (a) $(\frac{\lambda}{\omega_0})^2$ as a function of $x = \Omega/2\omega_0$ in both regimes (i) and (ii). The solid line is the parabola $(\frac{\lambda}{\omega_0})^2 = (\epsilon_f^2 - 1)x^2 + 2x - 1$, with $\epsilon_f = 3.3 \times 10^{-2}$. (b) Regime (ii): $\sin[2\,\mathrm{Arg}\{B_{\mathrm{exp}}(t \gg \lambda^{-1})\}]$ versus $1/x = 2\omega_0/\Omega$. The solid line is a fit: $\sin(\chi - \varphi)$ as a function of $1/x$, obtained with $\varphi = -0.29$ rad.

According to formulae (42) and (44), and equalling $\beta(t)$ and $\omega_0 t$ for first-order consistency again, we expect B_{exp} to follow the law

$$B_{\mathrm{exp}}(t) = (\alpha_{\mathrm{exp}+}(0)\,\mathrm{e}^{\lambda t} + \alpha_{\mathrm{exp}-}(0)\,\mathrm{e}^{-\lambda t})\mathrm{e}^{-\frac{\gamma}{2}t}. \tag{52}$$

Let us recall that, with our experimental device, dissipation is dominated by solid friction, so that the $\mathrm{e}^{-\frac{\gamma}{2}t}$ factor in equation (52) is not realistic. But the qualitative behaviour remains valid.

In figures 4(a) and (b), $\Omega = 2.13\omega_0$ and thus $\delta = 0.065\omega_0 > \Omega|c_1| = 0.035\omega_0$: we are in regime (i). The effect of length modulation is only to modulate the magnitude of the oscillations. In figure 4(b), we show the trajectory followed by B_{exp}, as calculated from the curve of figure 4(a). As expected in regime (i), λ is imaginary and B_{exp} follows a trajectory spiralling with the angular frequency $|\lambda|$.

In figures 4(c) and (d), $\Omega \simeq 2\omega_0$ and thus $\delta \simeq 0$: we are in regime (ii). The effect of modulation is 'strong'. In this example, the magnitude of the oscillations begins by decaying, then grows exponentially after a while. Figure 4(d) shows the trajectory of B_{exp} for this experiment. Let us analyse this trajectory. The experiment being performed near parametric resonance, we have $\chi \simeq 0$. Equations (49) thus yield $\alpha_+(0) = \mathrm{Re}\{\alpha(0)\}$ and $\alpha_-(0) = \mathrm{i}\,\mathrm{Im}\{\alpha(0)\}$. In figure 4(d), we can see that $|\mathrm{Re}\{B_{\mathrm{exp}}(0)\}| \ll |\mathrm{Im}\{B_{\mathrm{exp}}(0)\}|$. So $|\alpha_+(0)| \ll |\alpha_-(0)|$ and the $\mathrm{e}^{-\lambda t}$ term dominates. As a consequence, the magnitude of the oscillations decays. But since $\alpha_+(0)$ is not strictly zero, the $\mathrm{e}^{\lambda t}$ term finally becomes dominant, and the magnitude of the oscillations grows again exponentially. This asymptotic regime goes with a locking of the phase, which tends towards an asymptotic value, almost π in this example[7].

We can check that the agreement between theory and experiments is quantitatively good by measuring the values of λ and χ for different values of Ω.

Figure 5(a) shows the result for λ by displaying $\left(\frac{\lambda}{\omega_0}\right)^2$ as a function of $x = \Omega/2\omega_0$. Since $\lambda^2 = \Omega^2|c|^2 - \delta^2$, with $c = \frac{\epsilon_f}{2}$ and $\delta = \frac{\Omega}{2} - \omega_0$, the theoretical curve (solid line) is the parabola $\left(\frac{\lambda}{\omega_0}\right)^2 = \left(\epsilon_f^2 - 1\right)x^2 + 2x - 1$. One can appreciate the agreement between theory and experiment. Note that the way we measure λ depends on which regime is concerned. In

[7] Owing to (49), the asymptotic argument of $B_{\mathrm{exp}}(t)$ should be that of $\alpha_+(0)$, i.e. zero since $\mathrm{Re}\{\alpha_0\} > 0$. But figure 4(d) should be analysed keeping in mind that χ and φ are not exactly zero, as discussed below.

regime (i), λ is imaginary and we evaluate it by measuring the period of magnitude variations[8]. In regime (ii), λ is real and we evaluate it by a fit of the asymptotic exponential growth of the oscillation amplitude.

As for angle χ (defined by (48) in regime (ii) only), it can be derived from the measurement of the asymptotic argument of $B_{\rm exp}$ which is theoretically expected to be equal to $\frac{\chi-\varphi}{2}$ (see (42) and (49)). Figure 5(b) displays $\sin(\chi-\varphi) = \sin[2\,\mathrm{Arg}\{B_{\rm exp}(t \gg \lambda^{-1})\}]$ as a function of $1/x = 2\omega_0/\Omega$. If φ were exactly zero, we would obtain a straight line (see (48)). Actually the fit gives $\varphi = -0.29$ rad (solid line in figure 5(b)). This negative value indicates that the voltage peak we obtain on the coil occurs slightly *before* the cylinder reaches its mean position ($\ell_{\rm c} = \ell_{\rm c0}$). This is well explained if we account for the finite sizes of the coil (radius 2.5 cm) and the magnet (radius 1.4 cm). Indeed, the magnet-induced flux through the coil varies more significantly when both elements *begin to face each other* than when they are *exactly aligned* (i.e. maximum flux). Since the disc has a radius of 10 cm, the beginning of the {magnet–coil} face to face occurs for a rotation angle of the disc roughly $\frac{2.5+1.4}{10} \simeq 0.39$ rad *before* their exact alignment, as can be checked by glancing at figure 1(b). The $\varphi = -0.29$ rad value obtained with the fit fairly ranges between 0 and -0.39 rad, as expected.

6. Conclusion

In this paper, we have shown that use of the classical Glauber formalism leads to a very simple form for the harmonic oscillator dynamic equations. This is particularly true for the free oscillation, but holds too in the case of a weak viscous damping or a parametric excitation. Moreover, the simplicity of these dynamic equations suggests the relevant approximations to be made to solve them, as well as allowing complete resolutions. When considering parametric excitation for instance, the adiabatic invariant appears very naturally to be the semi-classical quanta number $|\alpha|^2$. The existence of the $\Omega = 2\omega_0$ resonance is also a very intuitive result, and the interpretation of experimental behaviour such as that displayed in figure 4(a) or (c) is particularly easy whereas it would probably be a brain-racking task without the α-formalism used in this paper. Of course, one could object that to profit by this more natural resolution of the problem, it is necessary to use the Hamiltonian formalism, which could *prima facie* seem to be handicapping from a pedagogical point of view. In our opinion, it is in fact a great asset: it gives one more reason to teach the Hamiltonian formalism in a purely *classical* framework, which provides a solid grounding for students who may later tackle quantum mechanics.

Acknowledgments

We acknowledge Patrick Lepers and Maurice Gilbert for their decisive contribution in realizing the experimental device.

References

[1] Ruby 1996 *Am. J. Phys.* **64** 39
[2] Berthet R, Petrosyan A and Roman B 2002 *Am. J. Phys.* **70** 744
Curzon F L, Loke A L H, Lefrançois M E and Novik K E 1995 *Am. J. Phys.* **63** 132
Fameli N, Curzon F L and Mikoshiba S 1999 *Am. J. Phys.* **67** 127
[3] Kittel C, Knight W D and Ruderman M A *Berkley Physics Course, Mechanics* (New York: McGraw-Hill) chapter 7
[4] Landau L and Lifschitz E 1960 *Mechanics* (London: Pergamon) section 27

[8] Note that in this regime, $B_{\rm exp}$ spirals with the angular frequency λ so that $|B_{\rm exp}|$ oscillates with the angular frequency 2λ.

[5] Brillouin L 1946 *Wave Propagation in Periodic Structures* (New York: McGraw-Hill)
Morse P M and Feshbach H 1953 *Methods of Theoretical Physics* (New York: McGraw-Hill)
[6] Glauber R J 1963 *Phys. Rev.* **131** 2766–88
Glauber R J 1965 Optical coherence and photon statistics *Quantum Optics and Electronics* (New York: Gordon and Breach)
[7] Cohen-Tannoudji C, Diu B and Laloë F 1977 *Quantum Mechanics* (New York: Wiley)
Merzbacher E 1998 *Quantum Mechanics* 3rd edn (New York: Wiley)
[8] Squire P T 1986 *Am. J. Phys.* **54** 984
Peters R D and Pritchett T 1997 *Am. J. Phys.* **65** 1067
Wang X J, Schmitt C and Payne M 2002 *Eur. J. Phys.* **23** 155
[9] Pippard A B 1978 *The Physics of Vibration* vol 1 (Cambridge: Cambridge University Press)
Ehrich F F 1976 Self-excited vibration *Shock and Vibration Handbook* ed C M Harris and C E Crede (New York: McGraw-Hill)
[10] Case W B and Swanson M A 1990 *Am. J. Phys.* **58** 463
Case W B 1996 *Am. J. Phys.* **64** 215